CHAPTER 6

IN-SITU DERIVATISATION ON SILICONE RUBBER TRAPS

6.1 IN-SITU DERIVATISATION

Low molecular mass aldehydes are both volatile and polar. In order to pre-concentrate them from the air, we must first convert them into thermally stable, less polar compounds. This is commonly achieved by using a derivatisation reaction, as described in chapter 2.

6.1.1 SELECTING A DERIVATISING REAGENT

A derivatising reagent can be split into two parts, namely the bulk organic substituent and the reactive substituent [127]. The bulk organic substituent should enhance the detector sensitivity to the product and simultaneously decrease the volatility of the product; it is responsible for providing a chemically and thermally stable product. However, this group should be carefully considered since the bulk can also sterically hinder the reaction, affecting the reaction rate. The reactive substituent determines the selectivity of the reaction, by reacting only with certain functional groups in the presence of others [127].

Of the several reagents that have been used for the derivatisation of aldehydes, as seen in chapter 2, O- (2,3,4,5,6-PentaFlouroBenzyl) Hydroxyl Amine hydrochloride (PFBHA) was chosen for this study based on the following reasons. The reactive substituent, the amine, reacts only with carbonyl functional groups. The reaction efficiency is > 80% for HCHO and other low molecular mass aldehydes [50].

However, the reaction rate decreases for longer, more complex aldehydes [50]. This is due to the size of the bulk substituent, the pentafluorobenzyl group, which hinders the approach of the amine toward the aldehyde.

The pentafluorobenzyl group provides enhanced detectability, especially when using an electron capture detector. A base peak (100%) of m/z ratio 181 is obtained by EI-MS for the oxime products formed, which is ideal for Selected Ion Monitoring (SIM) [17,22,50,54,55].

The oxime-product is thermally stable and volatile [17,22,50] therefore ideal for GC analysis. Comparisons of reagents in the literature [22] also indicate that PFBHA, unlike other reagents, displays only one peak on the chromatogram corresponding to the reagent. In addition, since similar work using SPME has been performed with this reagent [22] it would allow for a comparison of the results obtained when using the silicone trap.

The suggested mechanism for the reaction between an aldehyde and O - (2,3,4,5,6-PentaFluoroBenzyl) HydroxylAmine hydrochloride (PFBHA), is shown in figure 6.1.

6.1.2. THE SILICONE RUBBER TRAP

Derivatsation is performed *"in-situ"* meaning in the collection medium, in our case, the silicone rubber. The procedure for *in-situ* derivatisation on the silicone rubber trap is depicted in figure 6.2.

As discussed in chapter 3, there are several reasons why the silicone rubber trap is ideal for pre-concentrating pollutants. It is particularly suitable for *in-situ* derivatisation because it is inert and will not participate or inhibit the reaction between the aldehyde and the PFBHA. The only fragments produced through silicone degradation have repeatable retention times and are easily identified using Mass Spectrometry. Figure 6.3, shows a typical blank chromatogram of a silicone trap desorption run on GC-FID,

using the conditions in table 6.1, temperature program B. Typical mass spectral silicone degradation fragments are m/z 73, 207, 211 and 281. Sixteen-channel silicone rubber traps were used during this study; their preparation has previously been described by Ortner and Rohwer [24-27].

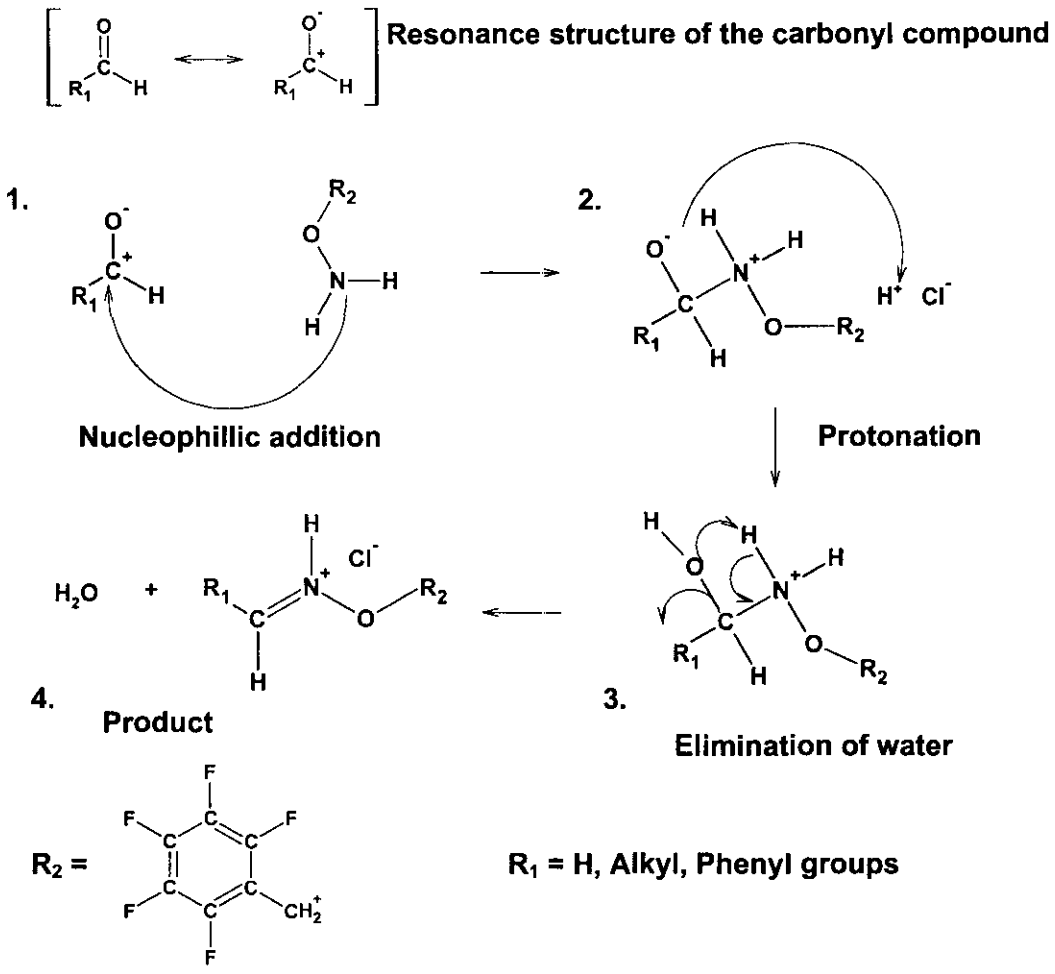

Figure 6.1. The suggested mechanism for the reaction of an aldehyde with PFBHA.

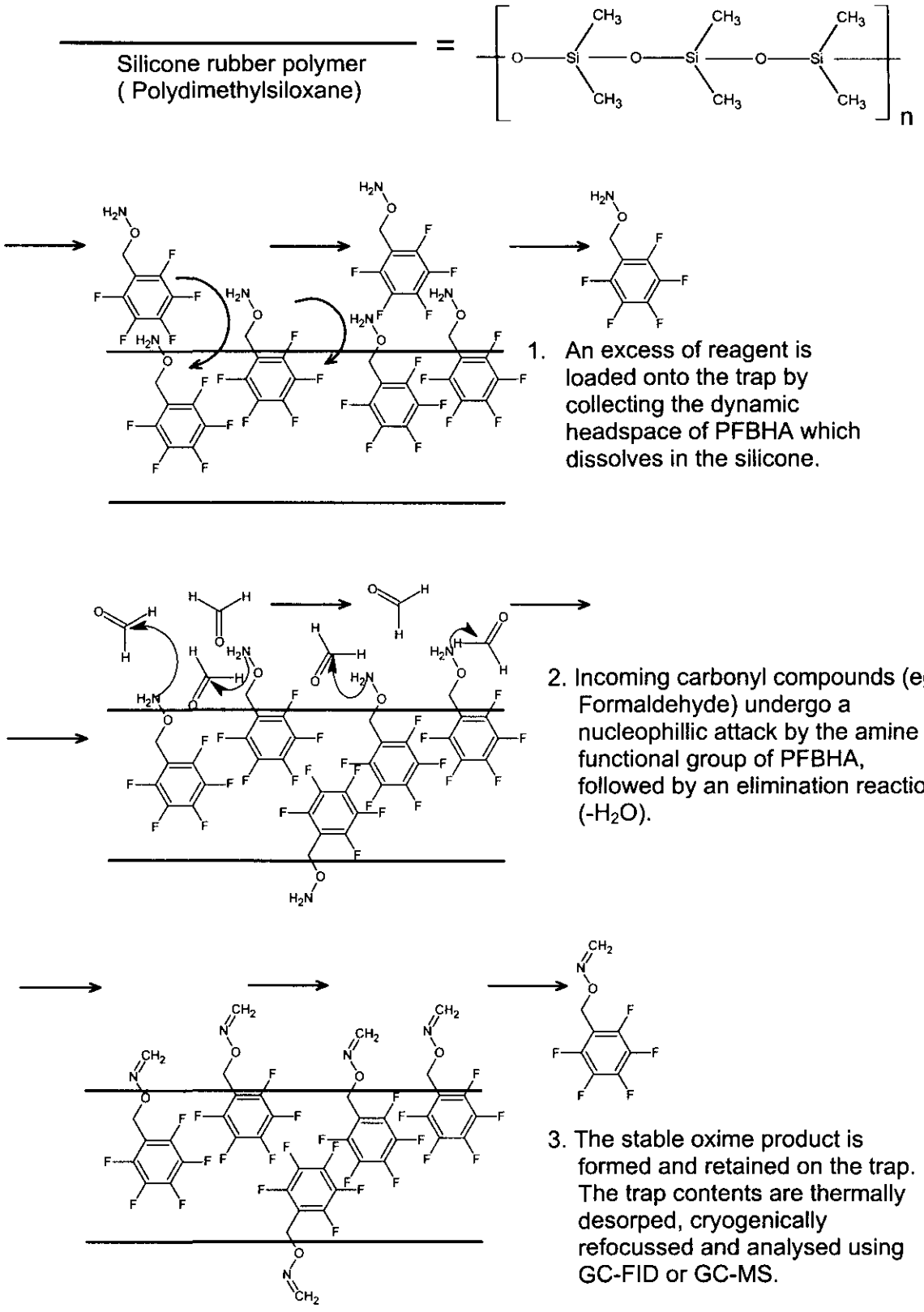

Figure 6.2. In-Situ derivatisation on the silicone rubber trap.

Table 6.1. Instrumentation Parameters.

TCT 4020 UNIT:	
ROD	250°C
PRECOOL	-100°C / 2min
DESORB	220°C / 15min
DESORB FLOW RATE	50 ml/min
INJECT	250°C / 1min
BACKFLUSH	280°C / 10min
BACKFLUSH FLOW RATE	60 ml/min
HP5890 GC:	
COLUMN	30m ZB-5, 0.25mm I.d., df 0.25µm
CARRIER GAS	Helium
VOLUME FLOW RATE	0.6ml/min
TEMPERATURE PROGRAM A	30°C / 1min // 5°C/min // 150°C //
	50°C/min // 280°C / 4min
TEMPERATURE PROGRAM B	30°C / 1min // 5°C/min // 280°C / 4min
TEMPERATURE PROGRAM C	80°C / 2min // 5°C/min // 180°C //
	40°C/min // 260°C / 2min
HP 5890 FID:	
FLAME GAS N2 : H2 : O2	20 : 60 : 300 ml/min
TEMPERATURE	300°C
RANGE	2^4
HP 5988 QUADRUPOLE MS:	
ION SOURCE TEMPERATURE	220°C
TRANSFER LINE TEMPERATURE	280°C
SCAN RANGE	40 - 400 amu
VARIAN 3300 GC:	
COLUMN	30m DB-5, 0.25mm i.d., df 0.25µm
CARRIER GAS	Helium
VOLUME FLOW RATE	0.4 ml/min
TEMPERATURE PROGRAM	30°C / 1min // 5°C/min // 150°C //
	50°C/min // 280°C / 4min
FINNIGAN MAT ION TRAP MS:	
ION SOURCE TEMPERATURE	150°C
TRANSFER LINE TEMPERATURE	220°C
SCAN RANGE	40 - 400 amu

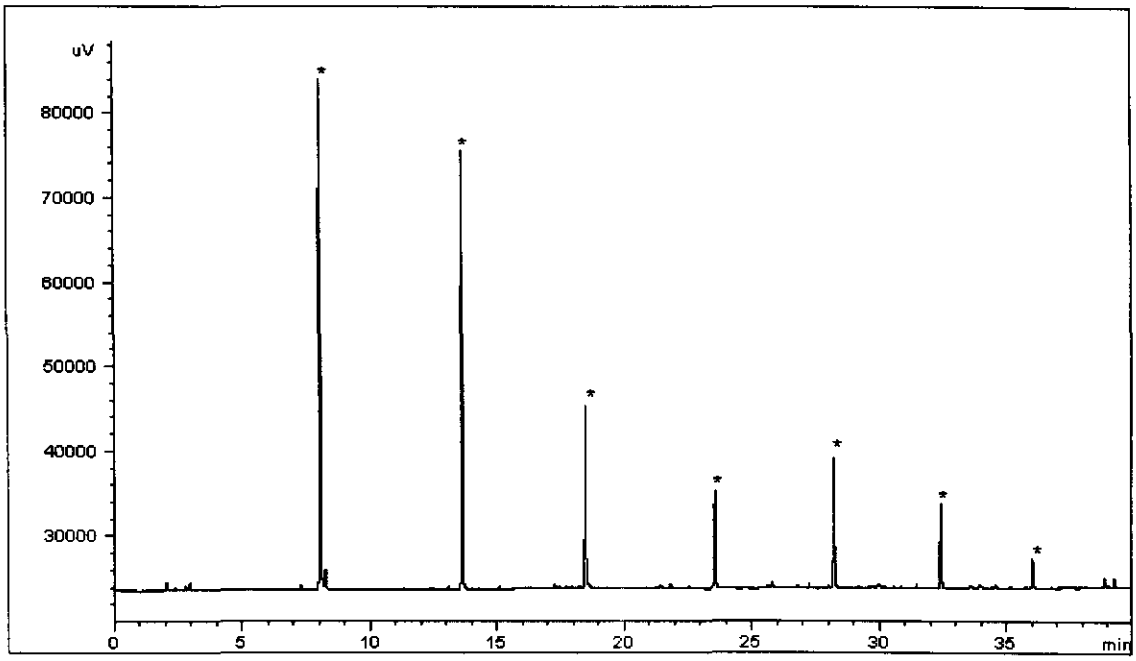

Figure 6.3. GC-FID chromatogram of a desorbed silicone rubber trap.

6.2 IDENTIFICATION OF THE REAGENT AND OXIME-PRODUCTS

A quick study was carried out in order to determine the mass spectra and elution order of the reagent and oxime products using a 100% PDMS SPME fibre. Reaction schemes for each aldehyde with PFBHA are shown in appendix 3, along with the product molecular formulas and masses.

The SPME fibre was exposed to the dynamic headspace of a 10g/L aqueous PFBHA solution, for 1min at a flow rate of 10ml/min, followed by exposure to the pure aldehyde for 10 seconds. This method was followed for each aldehyde. The fibre was desorbed in the inlet, splitless for 1min at 250°C, of the HP5890 GC followed by mass spectral analysis by a quadrupole mass analyser. Temperature program C in table 6.1 was used. Figure 6.4, shows the elution order of the aldehydes, except for the HCHO-oxime and PFBHA, which elute before acetaldehyde, as shown in figure 6.12 and figure 6.16.

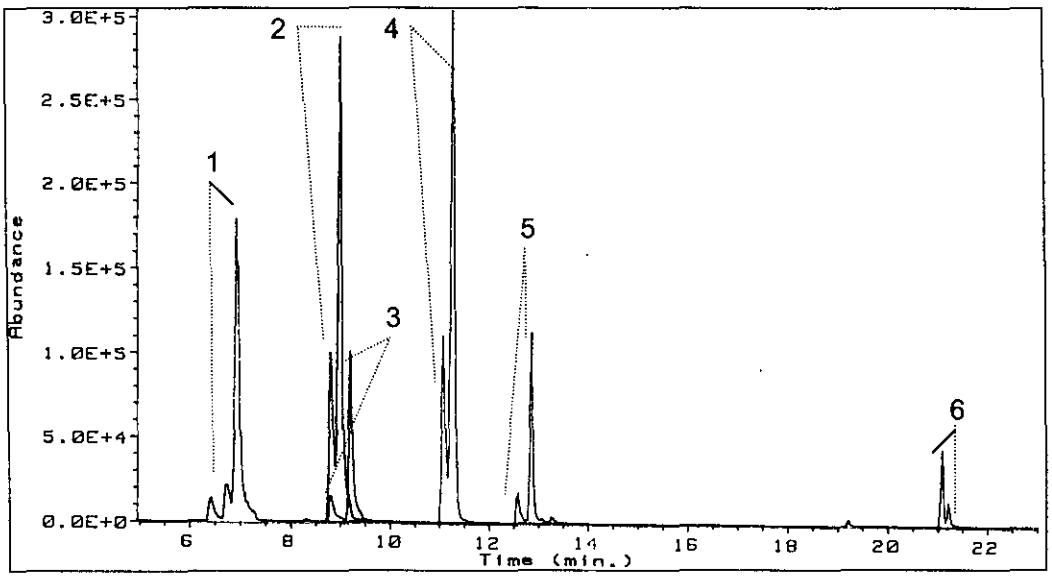

1. Acetaldehyde-oxime 2. Propanal-oxime 3. Acrolein-oxime
4. Butanal-oxime 5. Crotonal-oxime 6. Benzaldehyde-oxime

Figure 6.4. Overlaid TIC of SPME-PFBHA coated fibre exposure to pure aldehydes.

Non-symmetrical carbonyl groups will form E/Z isomers around the carbon-nitrogen double bond [50,128,129]. From the chromatogram, figure 6.4, we observed separated isomers for propanal, acrolein, butanal, crotonal and benzaldehyde. In our study, both peaks were integrated for quantitation.

Propanal and acrolein co-elute, but a separation can be achieved, if desired, by using a mass spectrometer, and selecting the m/z ratios unique to each compound, namely m/z 236 for propanal and m/z 250 for acrolein.

Mass spectra for the PFBHA, formaldehyde-oxime and acetaldehyde-oxime obtained, along with the corresponding NIST (National Institute for Standards and Technology) mass spectrum are shown in figure 6.5, 6.6 and 6.7 respectively. The mass spectra for other aldehydes studied can be found in the appendix 4. Table 6.2, lists the main mass spectral fragments for each aldehyde-oxime studied, obtained on the quadrupole MS. Where possible, these have been compared to literature values.

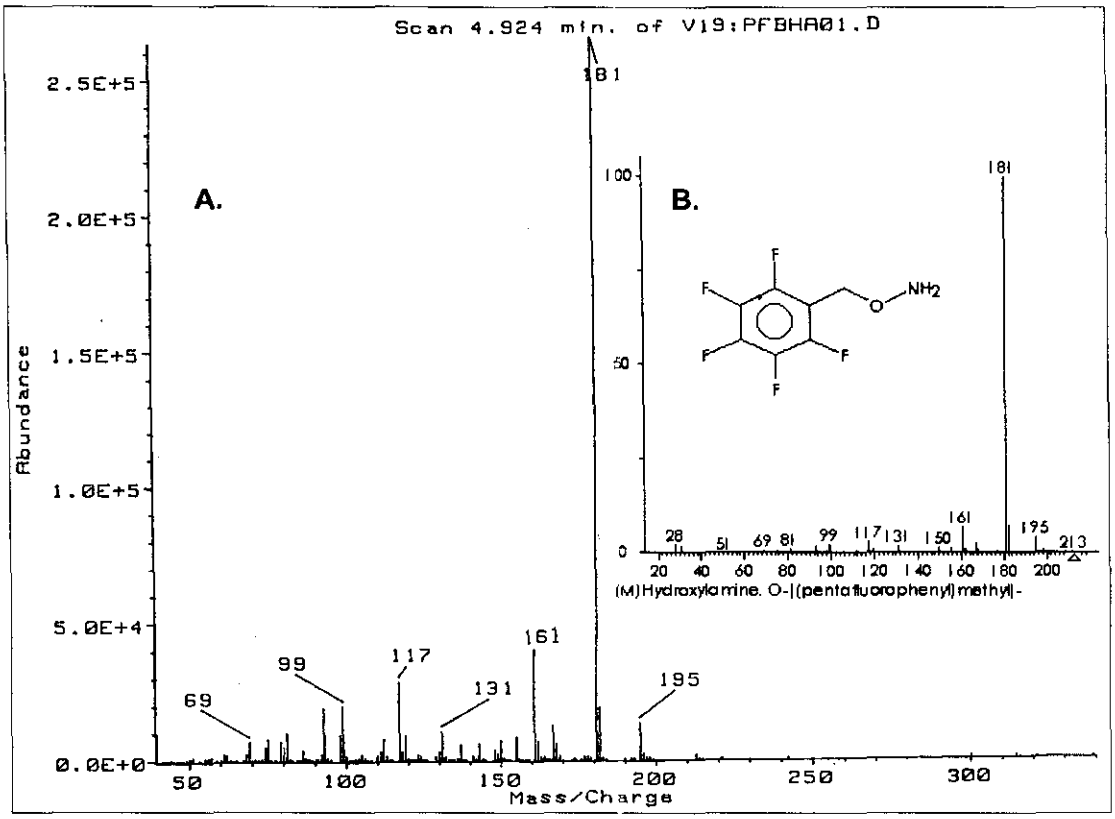

Figure 6.5. **A.** Obtained EI-Mass Spectrum for PFBHA.
B. NIST library EI-Mass Spectrum for PFBHA .

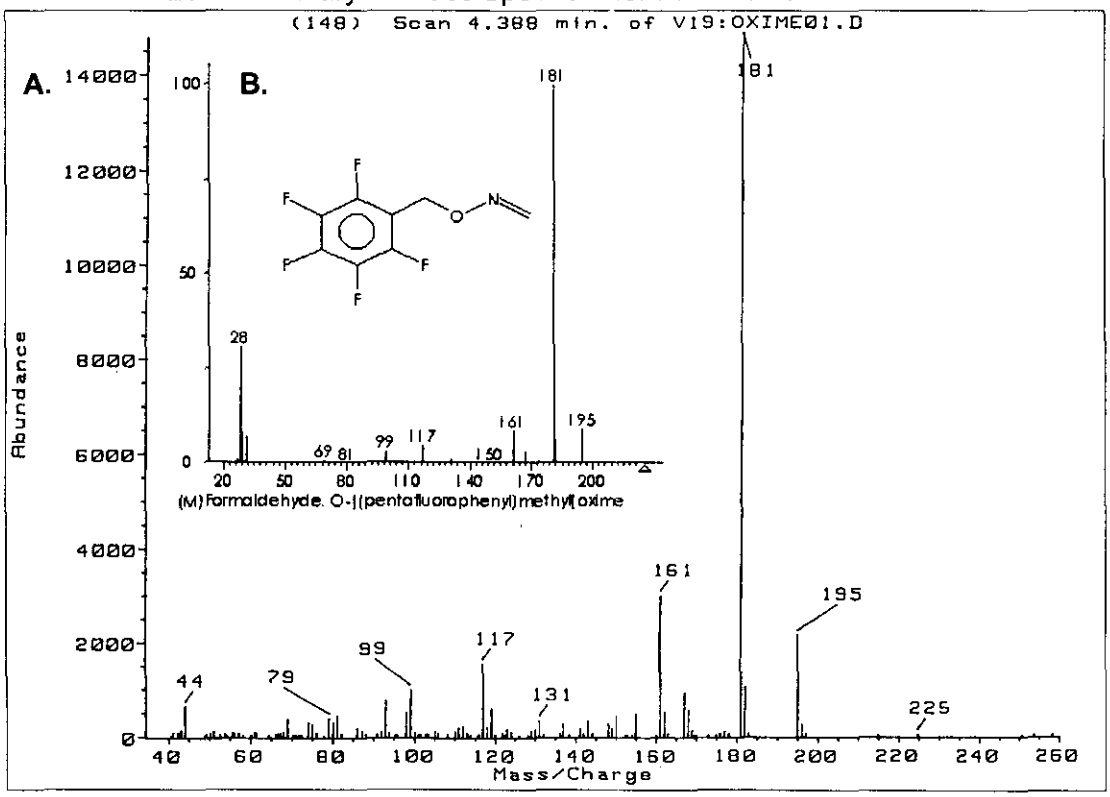

Figure 6.6. **A.** Obtained EI-Mass Spectrum for HCHO-Oxime.
B. NIST library EI-Mass Spectrum for HCHO-Oxime.

Table 6.2. EI-Mass spectra for PFBHA-aldehyde derivatives.

Compound	Molecular mass		m/z Relative abundance									Description:
	compound	PFBHA - oxime										
Formaldehyde	30	213	$[M]^{+\bullet}$	181	195	161	117	182	99	167	93	
				100	11	10	9	7	7	5	5	Pure oxime - liquid injection [50]
				100	12	10	9.9	6.7	9.6	5.4	6.3	Pure oxime - liquid injection [22]
				100	9.1	8.7	4.8	6.5	3.3	3.3	0.6	NIST
				100	**15.8**	**15.5**	**9.7**	**7.4**	**7.3**	**2.7**	**4.2**	**experimental EI-ITD**
				100	**12.1**	**9.7**	**6.7**	**7.7**	**4.9**	**4.5**	**3.7**	**experimental EI-QUADRUPOLE**
Acetaldehyde	44	239	$[M]^{+\bullet}$	181	195	161	117	182	209	167	99	
				100	6	6	5	7	8	4	4	Pure oxime - liquid injection [50]
			3	100	4	3	2	9	11	3		PFBHA-oxime formed in beer [22]
				100				0.6	1.3			NIST
			1.5	**100**	**3.5**	**6.8**	**5.4**	**7.1**	**6.0**	**3.5**	**4.6**	**experimental EI-QUADRUPOLE**
Propanal	58	253	$[M]^{+\bullet}$	181	195	161	117	182	223	236		
			1.2	100	3.7			7.1	5.5	8.6		Pure oxime - liquid injection [50]
			3	100	4	3	2	9	7	9		PFBHA-oxime formed in beer [17]
			0.8	100	3.4	3.6	1.6	7.6	6	9.4		NIST
			0.6	**100**	**3.3**	**4.9**	**4.3**	**8.4**	**2.1**	**10.1**		**experimental EI-QUADRUPOLE**
Acrolein	56	251	$[M]^{+\bullet}$	181	195	161	117	182	250	99	42	
			4.8	**100**	**3.1**	**5.2**	**4.2**	**8.3**	**6.8**	**4.1**	**2.1**	**experimental EI-QUADRUPOLE**
			$[M]^{+\bullet}$	181	195	167	250	182	239	99	41	
Butanal	72	267		100	7	3	6	10	14	3	4	PFBHA-oxime formed in beer [17]
			0.4	**100**	**5.8**	**2.3**	**3.7**	**7.9**	**6.0**	**3.1**	**8.0**	**experimental EI-QUADRUPOLE**
Crotonal	70	265	$[M]^{+\bullet}$	181	195	161	117	182	250	251	43	
			1.0	**100**	**2.8**	**3.9**	**3.6**	**7.3**	**20.3**	**5.4**	**9.9**	**experimental EI-QUADRUPOLE**
Benzaldehyde	106	301	$[M]^{+\bullet}$	181	77	69	103	182	271	51	65	
			7.4	**100**	**17.0**	**9.0**	**8.5**	**7.5**	**5.3**	**14.6**	**13.5**	**experimental EI-QUADRUPOLE**

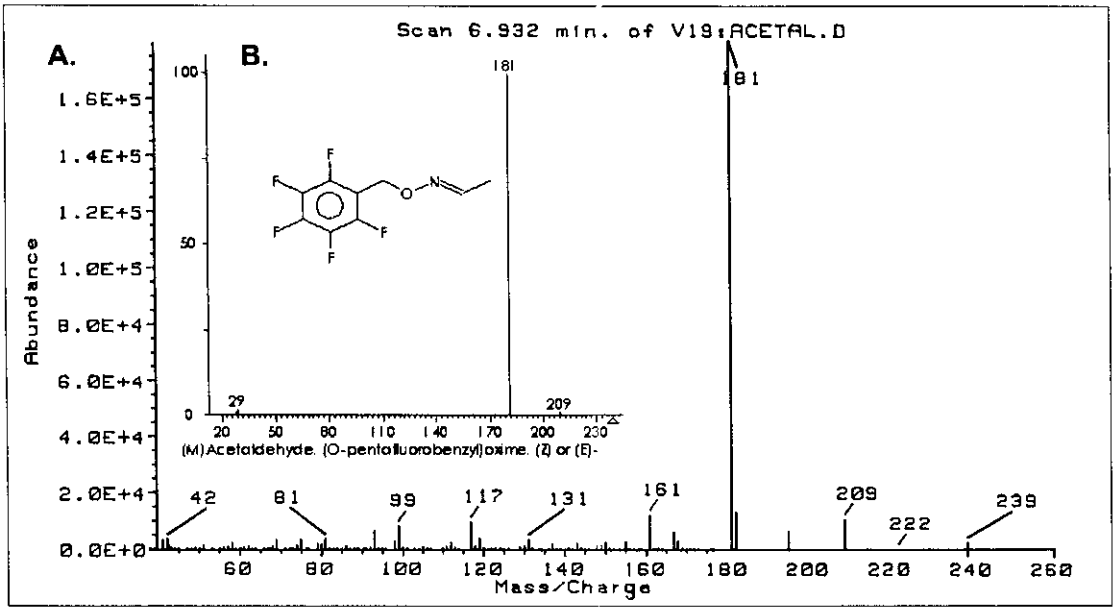

Figure 6.7. **A.** Obtained EI-Mass Spectrum for the acetaldehyde-oxime.
B. NIST library EI-Mass Spectrum for the acetaldehyde-oxime.

All oximes produce a base peak of m/z 181, which corresponds to the pentafluorotropylium ion, formed by the cleavage of the bond in the β–position to the pentafluoro-benzene ring [50,125]. Figure 6.8, demonstrates the formation of the pentafluorotropylium ion from the PFBHA-aldehyde derivative.

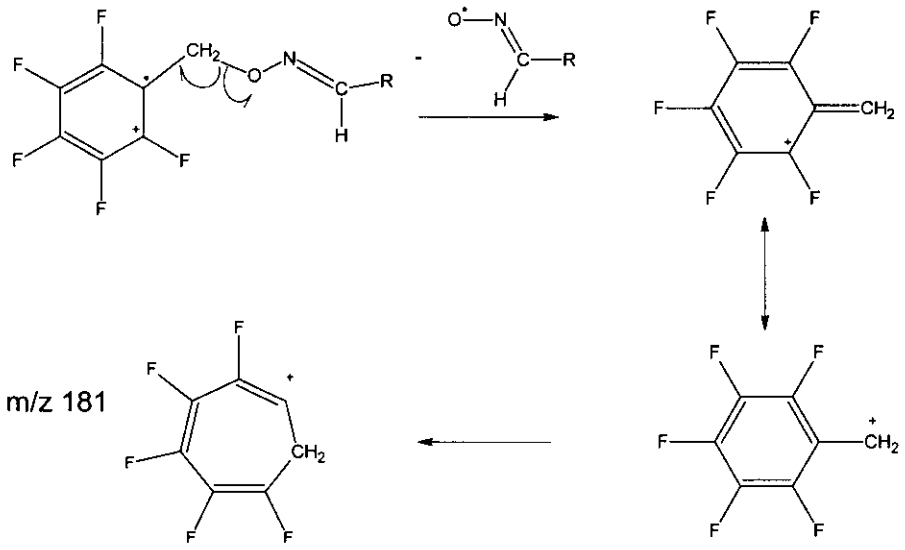

Figure 6.8. Formation of the pentafluorotropylium ion m/z 181 [50,125].

However, most PFBHA derivatives, excluding aldehydes that have an α, β double bond (acrolein, crotonal), afford very poor, often absent, molecular ions, which make the deduction of M^+ difficult [130].

Longer chain aliphatic aldehydes, C4 and longer, form PFBHA-oximes that produce an m/z 239 resulting from a McLafferty rearrangement [130], as demonstrated in figure 6.9 for the butanal-oxime. The m/z 239 ion was observed for our butanal-oxime, see appendix 4 and table 6.2.

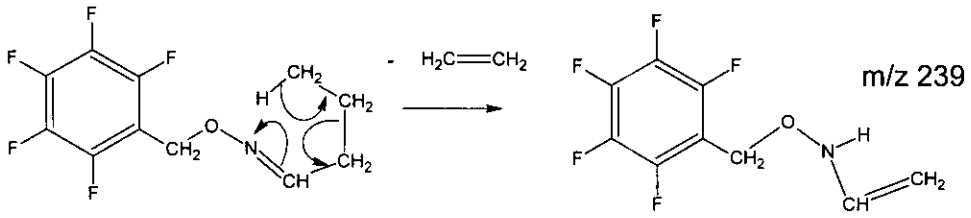

Figure 6.9. McLafferty rearrangement of the butanal-oxime to form m/z 239 [130].

The ion m/z 250 is predominant in most α, β double bond aldehydes. Spiteller et.al. [130], have suggested a mechanism for the generation of m/z 250, as depicted in figure 6.10.

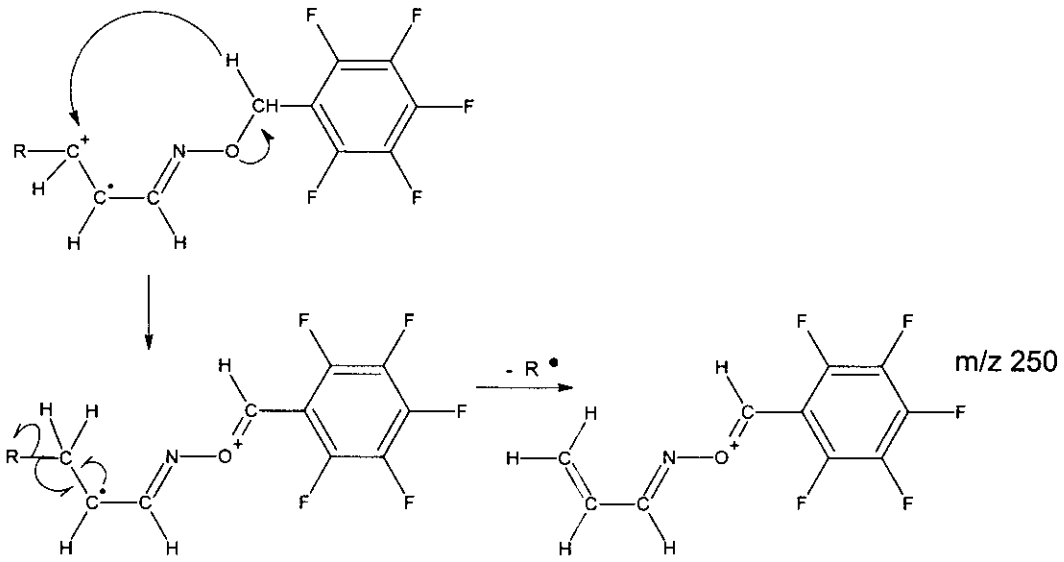

Figure 6.10. Mechanism for the formation of m/z 250 from 2-alkenal-oximes, where R• = H (acrolein) and CH_3 (crotonal) [130].

The ionised molecule undergoes a hydride migration from the benzylic hydrogen to the positive carbon atom, followed by carbon-carbon cleavage and the formation of a double bond. Both mass spectra for acrolein and crotonal display the m/z 250 ion, see appendix 4 and table 6.2.

Other ions formed are m/z 167, 155, 93 and 62 corresponding to the $C_6F_5^+$, $C_5F_5^+$, $C_3F_3^+$ and $C_2F_2^+$ ions, respectively. The abundances for these ions are below 5% for most aldehyde-oximes [50], as was also observed in our study.

Short chain aldehyde-oximes, such as acetaldehyde and propanal show the m/z [M - 30]$^{+\bullet}$, formed by the loss of NO from M^+[50]. Our acetal and propanal-oximes, displayed the m/z 209 and 223 respectively, corresponding to the suggested loss of NO [M - 30]$^{+\bullet}$.

Longer chain aldehydes will show a hydrocarbon pattern with successive losses of m/z 14 in the lower mass range of the mass spectrum [50]. For the benzaldehyde-oxime, m/z 77 and m/z 105 were observed representing the benzene and benzaldehyde ions respectively (see appendix 4).

With this information available, we could also test the permeation and diffusion standards prepared at the time. Figure 4.5 And 4.6 show the reconstructed ion chromatograms of m/z 181 for exposure of the SPME fibre for 5 and 10 min to the diffusion standards and permeation standards respectively.

6.3 THE DERIVATISING REAGENT

6.3.1 LOADING THE REAGENT ONTO THE SILICONE RUBBER TRAP

Methods commonly used to coat sorbents involve coating the sorbent with a solution containing the reagent followed by additional steps to remove the solvent [54,55]. We decided against this technique first, because it would be tedious and time consuming. Second, should all the solvent not be totally removed (particularly if the solvent is water) this would lead to deterioration of the column, the Mass Spectrometer ion source filament and extinguishing of the flame on the Flame Ionisation Detector. Instead, based on previous work by Martos and Pawliszyn [22] on SPME fibres, we decided to load the headspace of the PFBHA from an aqueous solution onto the trap, as this would preclude these disadvantages.

6.3.2 LOADING FROM AN AQUEOUS SOLUTION OF REAGENT

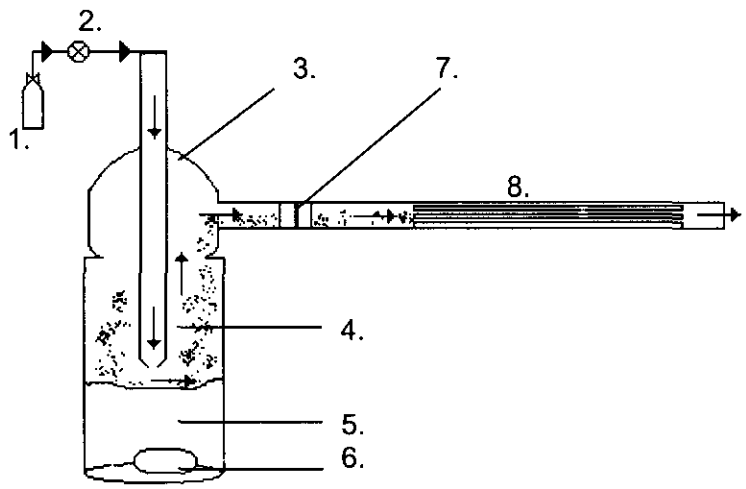

1. High purity nitrogen gas.
2. Mass flow controller.
3. Glass impinger.
4. Headspace of the reagent.
5. Aqueous reagent solution.
6. Glass coated stirrer.
7. Teflon tube connection.
8. Silicone rubber trap.

Figure 6.11. Set-up for loading headspace from aqueous reagent.

Figure 6.11, shows the set-up used. A 10g/L aqueous solution of PFBHA was prepared in 4ml of MilliQ water. Initially, the solution was placed in a fritted glass bubbler, without a magnetic stirrer. However, we found that this technique led to increased amounts of water condensing in the silicone trap, during collection. An impinger was used instead. The amount of solution was such that the nozzle was just above the surface of the solution. A glass-coated stir-bar was used to stir the solution at 250 rpm, while nitrogen gas was blown over the surface of the stirred solution, at a flow rate of 10ml/min. The dynamic headspace of PFBHA was collected for 30 seconds.

Thermal desorption and analysis of the trap, using a Varian GC - Finnigan Mat ITD, showed that the reagent was successfully loaded. Table 6.1, shows the experimental conditions used and figure 6.12, shows the chromatogram obtained for the collection of a 5 ppm HCHO atmosphere collected at a flow rate of 10ml/min for 10 seconds.

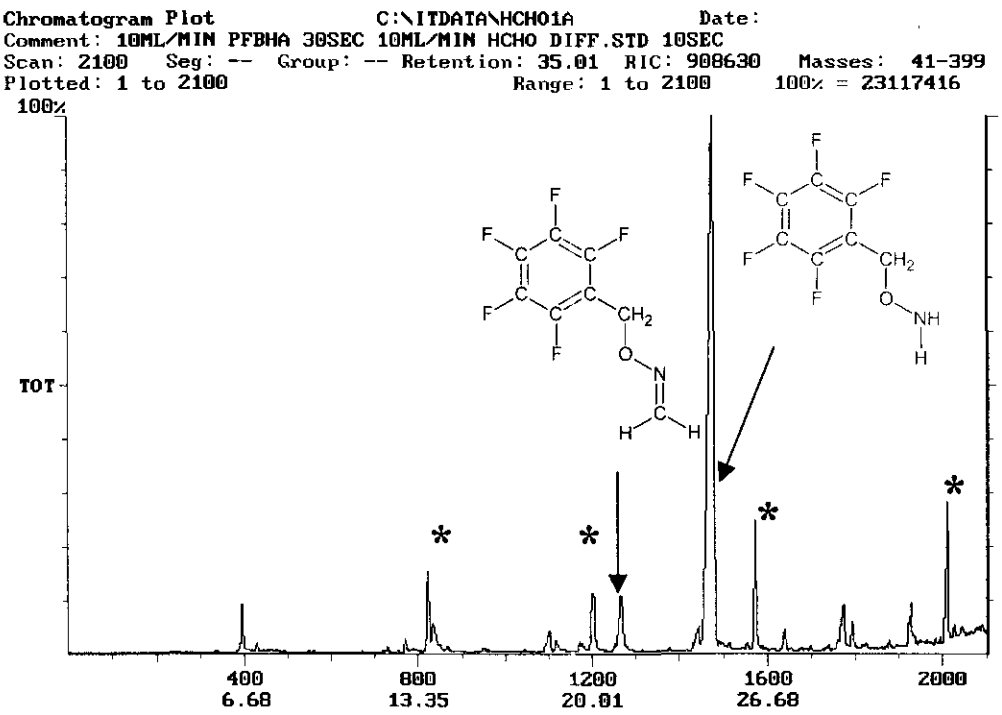

Figure 6.12. GC-ITD MS Total Ion Chromatogram of PFBHA (loaded from aqueous headspace) and 30sec sampling of a 5ppm HCHO atmosphere.

This set-up proved problematic, as discussed below.

Although silicone rubber is hydrophobic in nature, micro-litres of water collected on the trap. This amount of water, in combination with the excessive amount (micrograms) of reagent entering the ion trap contributed to the deterioration of vacuum conditions inside the Ion trap (ITD). The instrument could not be used further until the vacuum was restored and most of the water removed, this procedure can take up to two whole days. Removal of water from an ion trap is made difficult by the fact that the ion trap is held at a lower temperature (150°C) than, for example, the quadrupole mass analyser (250°C). In addition, because ions are held in the ion trap before mass separation, M+1 peaks were produced as a result of self chemical ionisation protonation. Figure 6.13, shows the mass spectrum for the HCHO-oxime obtained from the EI - ITD.

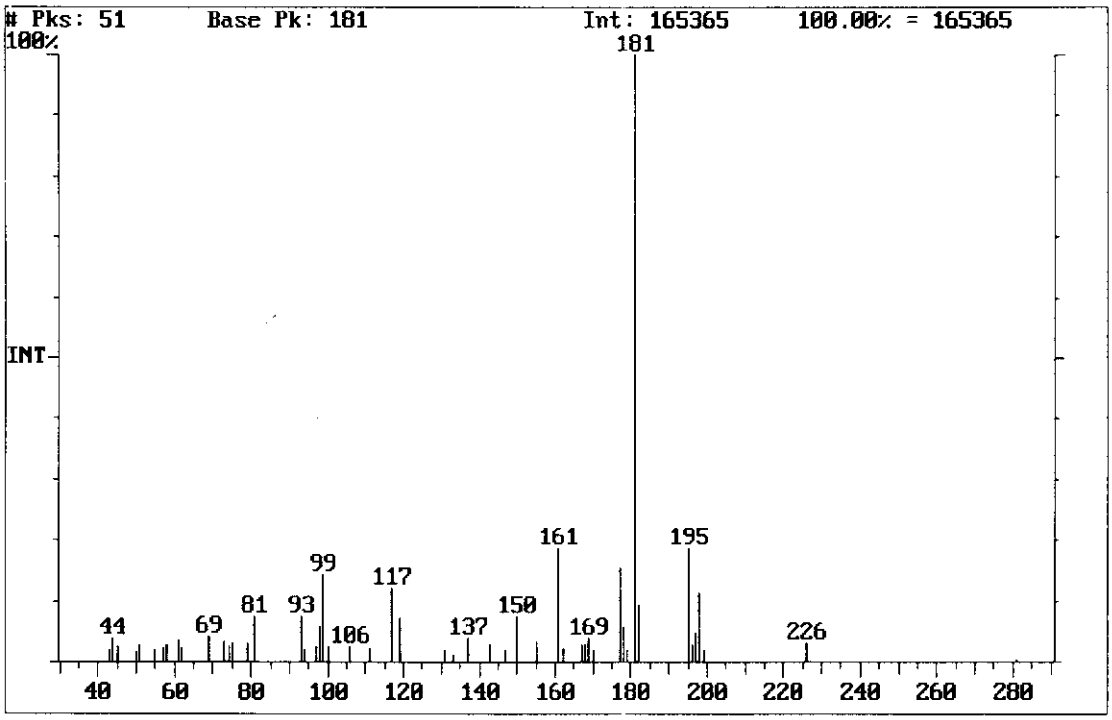

Figure 6.13. ITD EI-Mass spectrum of the formaldehyde-oxime.

Hence, we decided that the quadrupole mass analyser would be more suitable for any further mass spectrometry in this study.

In addition, prevention of excess water condensation in the silicone rubber trap could be achieved by keeping the temperature of the PFBHA aqueous solution a few degrees lower than the temperature of the trap. This was made possible by placing the impinger in a water-bath containing ice. The temperature was reduced from 18°C to 12°C. However, the repeatability of temperature for each PFBHA collection is difficult to maintain in this way.

6.3.3 REAGENT PURITY

We found formaldehyde-oxime contamination in the reagent blank. This is a serious problem experienced by several other users of PFBHA [51,128,129] and derivatisation reagents in general (chapter 2). Suggested reasons for this are first, HCHO is a by-product of ozonated water [51]. Second, HCHO is present in air which then dissolves in water [51]. Bidistilled, analytical reagent water, $KMnO_4$ oxidised and Milli-Q/ MilliPore water all contain the HCHO-Oxime [51,129], with the tandem Milli-Q system providing the lowest blank value [129]. Preliminary work showed that distilled water and Milli-Q water, in our labs, also displayed the oxime blank. The percentage of HCHO-Oxime relative to PFBHA collected is shown in figure 6.14.

The reagent blank is reported in this manner as the amount of oxime loaded appears to be proportional to the amount of PFBHA loaded, which is not a repeatable process (see section 6.3.5). However, since no amount of water purification could completely remove the HCHO-Oxime in the reagent blank, we decided to collect the headspace from the pure reagent, as this would surely remove the contamination present due to water.

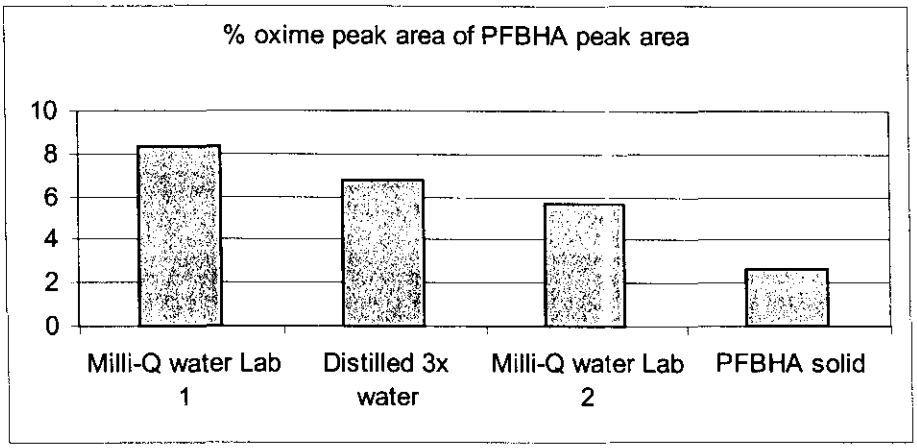

Figure 6.14. Comparison of HCHO-oxime in PFBHA (aq) and PFBHA (s).

6.3.4 LOADING FROM THE PURE REAGENT

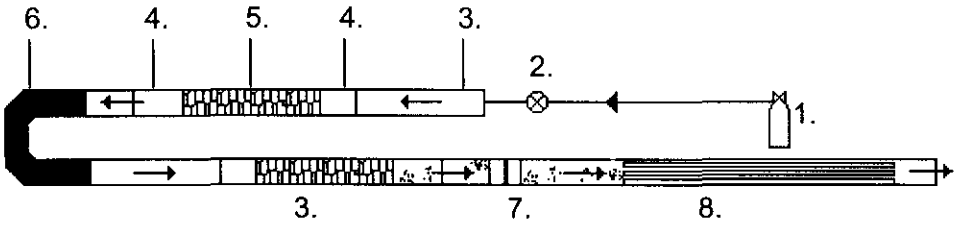

1. High purity nitrogen gas.
2. Mass flow controller.
3. Glass tube packed with reagent.
4. Glass wool plug.
5. Pure solid reagent.
6. Activated charcoal trap.
7. Teflon tube connection.
8. Silicone rubber trap.

Figure 6.15. Set-up for loading headspace from the pure reagent.

A PFBHA pre-trap and activated charcoal trap were included in the set-up to ensure that no trace amounts of HCHO potentially present in the nitrogen gas could enter the PFBHA loading trap. Any HCHO arising from the nitrogen gas would be derivatised by the first PFBHA trap and then trapped by the activated charcoal before reaching the tube containing the PFBHA from which the headspace would be concentrated in the silicone rubber trap. Figure 6.15, shows the set-up used. All collections were made at a room temperature of 22°C, maintained by air-conditioning in the lab. From the results obtained, it is clear that the reagent is also contaminated. Hence, we had to determine the reagent blank. An acceptable reporting method is to take the

average HCHO amount in a series of blanks plus 3 times the standard deviation for the series of blank runs [129]. This results in a reagent blank value of 23ng HCHO in a 10min collection of PFBHA at a flow rate of 5ml/min (n=5).

Figure 6.16, shows a GC-FID chromatogram of a typical reagent blank collected using this set-up.

6.3.5 REAGENT LOADING REPEATABILITY

At the start of the study it was not necessary to know precisely how much reagent was on the trap as long as it was present in excess. However, with the introduction of the reagent blank it became important that the amount of HCHO-oxime remain constant, as this would determine the detection limit for HCHO.

To study the collection from an aqueous solution of PFBHA (section 6.3.2), the silicone rubber trap was used to collect the dynamic headspace of PFBHA for 1 min at a flow rate of 10ml/min. Nitrogen gas would then be blown over the solution for a time and then another silicone trap would be loaded. This method was followed several times. All traps were analysed using the TCT4020 HP GC-FID instruments, with the parameters used described in table 6.1, using temperature program A and FID range 2^0. A repeat collection of PFBHA was performed the following day under the same conditions.

Figure 6.17, shows the curve for all the PFBHA (aq) collections over time.

From the repeated aqueous PFBHA collection a similar trend was noted. Namely, there is first a steep increase followed by a steady decrease in the amount of PFBHA collected. This could be due to the PFBHA first coating the inside of the glass vessel surfaces and then moving towards the trap, after which the vapour pressure of the PFBHA begins to decline.

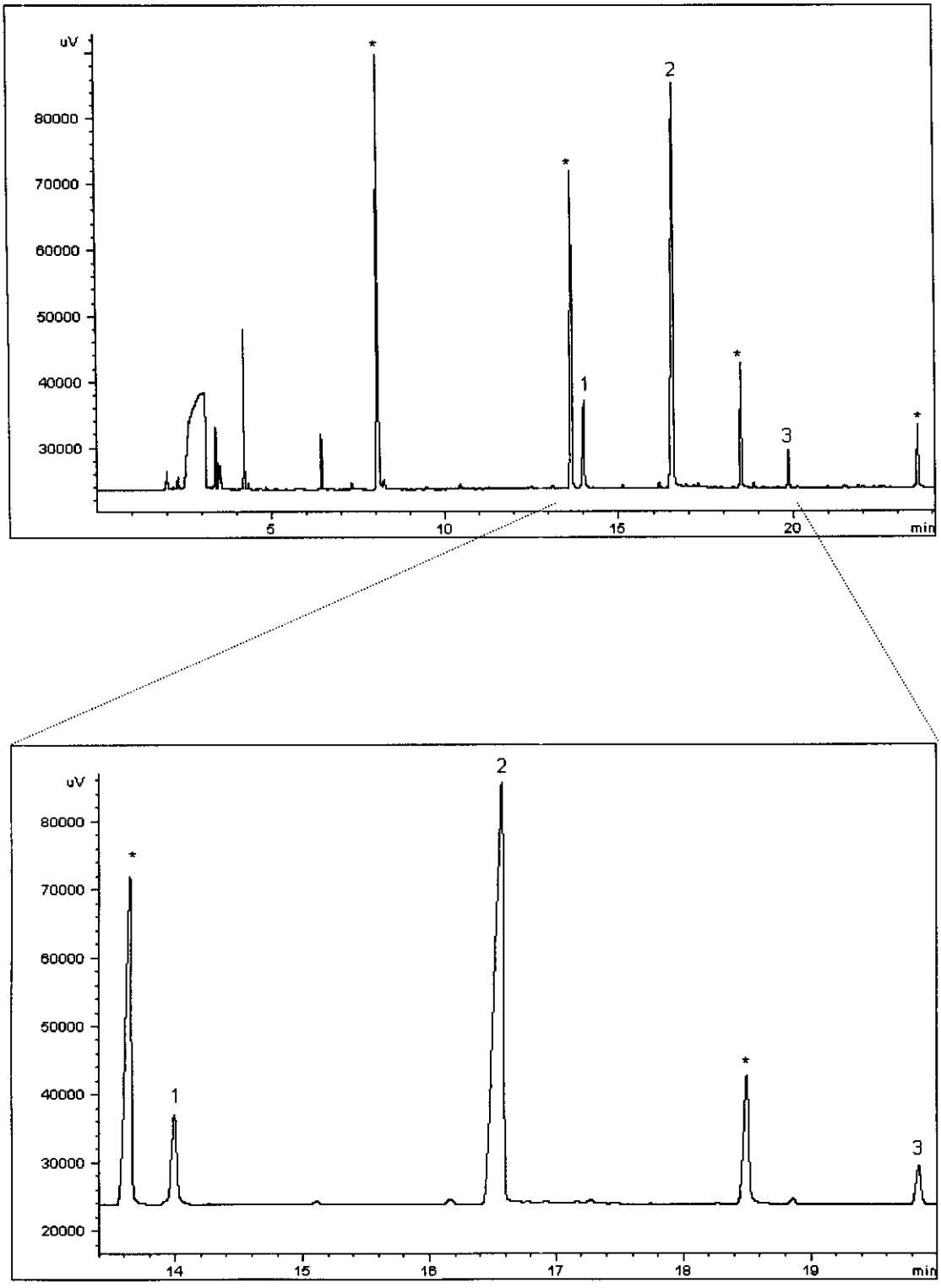

* Silicone peaks
1. Formaldehyde – oxime
2. PFBHA
3. 20ng C12

Figure 6.16. GC-FID chromatogram of the PFBHA reagent, headspace collected from the pure solid for 10min at 5ml/min.

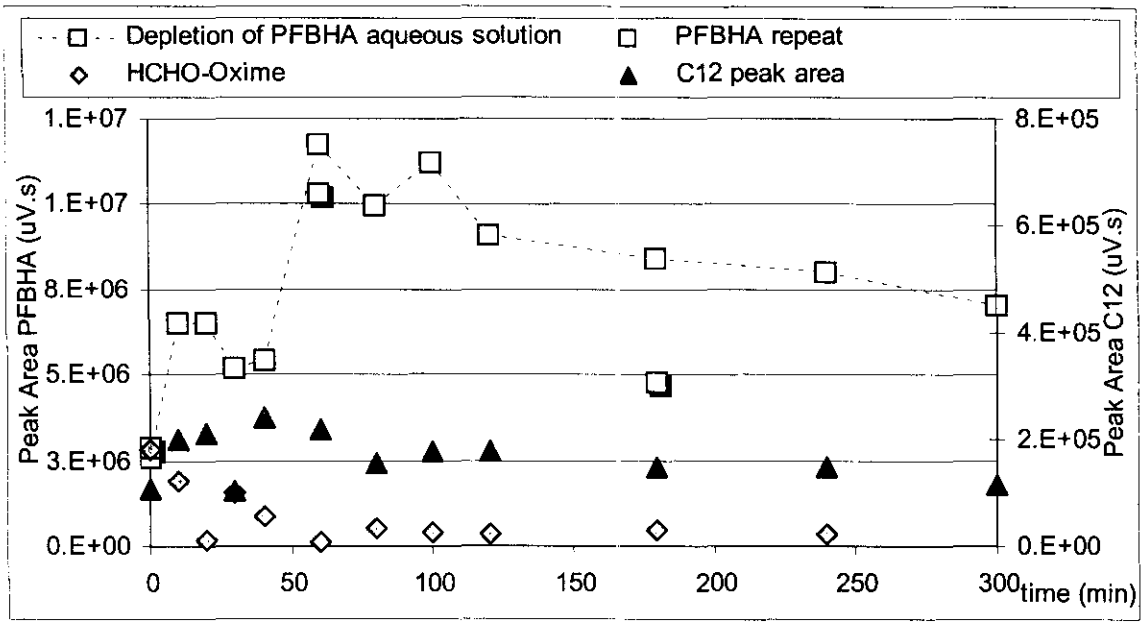

Figure 6.17. The depletion of PFBHA headspace from an aqueous solution.

A similar study was performed on the collection of PFBHA from the pure reagent (section 6.3.4). Silicone rubber traps were loaded with the headspace of PFBHA, as described in 6.3.4, for 10min at a collection flow rate of 10ml/min. They were loaded one after the other, except for the last trap which was loaded the next day. Instrumental conditions are described in table 6.1, using the TCT4020 HP GC-FID instruments, temperature program A and FID range 2^4. Results shown in figure 6.18.

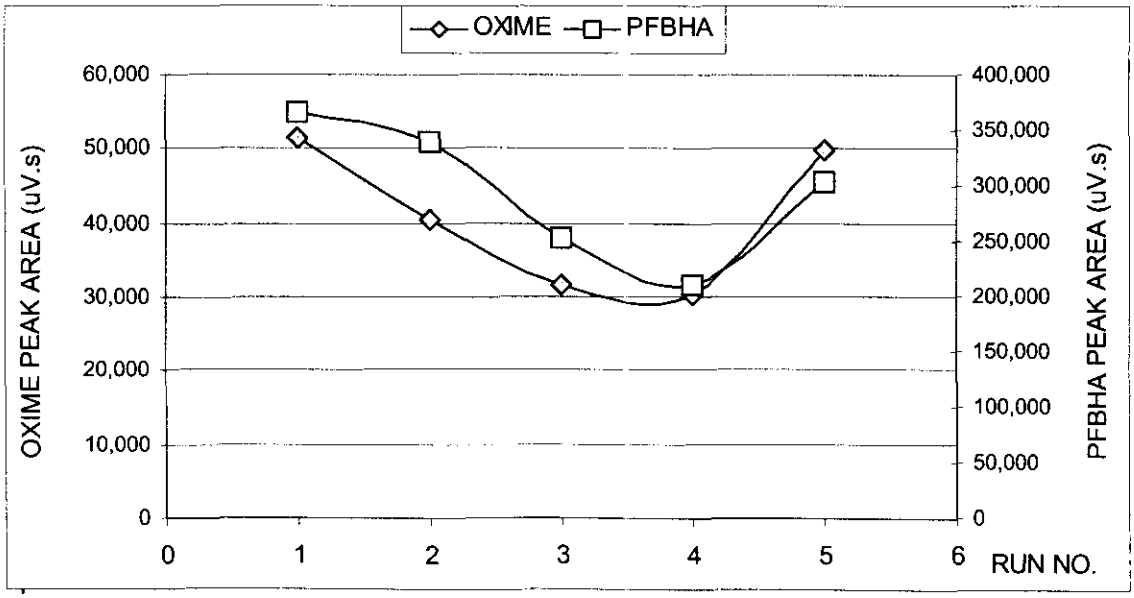

Figure 6.18. The depletion of PFBHA headspace from the pure reagent.

Figure 6.18, shows that the oxime amount changes proportionally with the amount of reagent loaded. Again, we noted that the amount of reagent collected decreases with every collection. However, the last data point is higher again, as this trap was loaded the following day. It would appear that the vapour pressure of the PFBHA decreases with every collection, and increases again over time when no collections are made. This was also observed with the aqueous PFBHA headspace collections.

It was becoming increasingly obvious that loading the reagent repeatably would be a problem. Since we decided not to collect PFBHA from the aqueous solution, a closer look at collecting from the pure reagent was made. Perhaps, by decreasing the collection flow rate from 10ml/min to 5ml/min, we could increase PFBHA loading repeatability.

A series of PFBHA collections from the pure reagent were made, at both flow rates, for increasing amounts of time. All traps were analysed using the TCT4020 HP GC-FID instrument parameters in table 6.1.

Figure 6.19, shows the increase in PFBHA and HCHO-oxime peak area with increasing loading volume at 5ml/min and 10ml/min. From the graph, it would appear that loading at a flow rate of 10ml/min seems ideal. It appears that more PFBHA is loaded at 10ml/min than at 5ml/min. However, the variation of the oxime peak area relative to PFBHA peak area is reduced from 67 % RSD to 19% RSD when moving from a collection flow rate of 10ml/min to 5ml/min, respectively. Thus using a collection flow rate of 5ml/min for reagent loading would provide more certainty on the amount of HCHO-Oxime already present in the reagent, before sample collection. However, from the graph, it is also clear that the amount of reagent loaded is greatly reduced at this flow rate. We are therefore limited to short sample collection times, as the reaction rate is dependent on an excess presence of reagent [22]. The collection volume can of course be extended if only trace amounts of aldehydes are present and the reagent is not depleted.

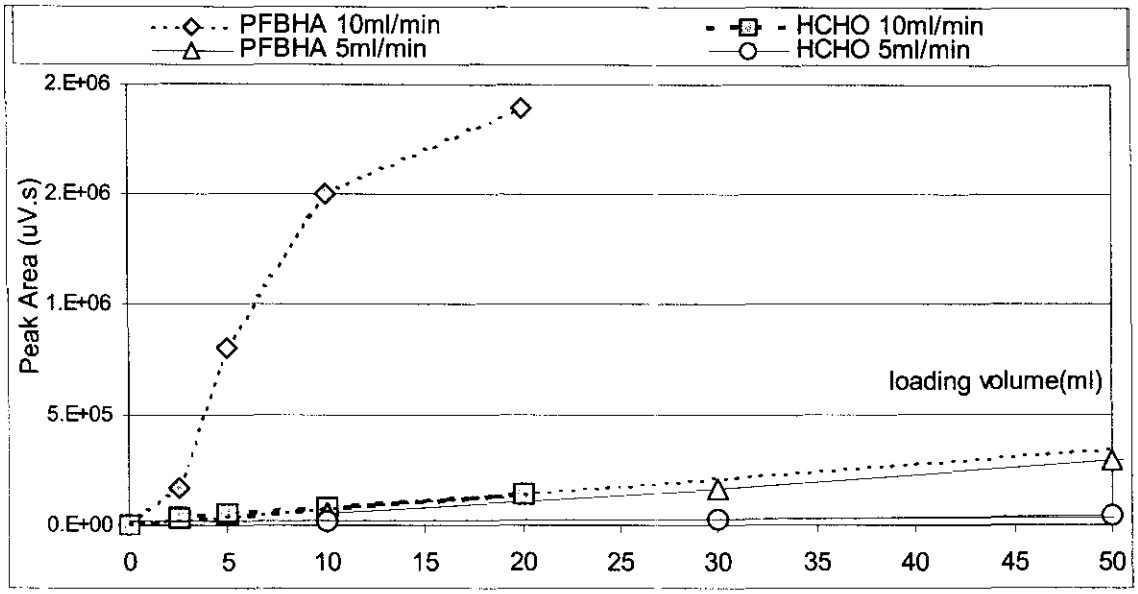

Figure 6.19. Peak area of PFBHA and HCHO-oxime with increasing loading volume at 5 and 10ml/min collection flow rates.

Martos and Pawliszyn [22], demonstrated, during their fibre selection process, by blowing nitrogen over the fibres, that the PFBHA is not as well retained on the 100% PDMS fibre as on their more polar variations. This was also observed on the silicone rubber trap, as shown in Figure 6.20, that the PFBHA depletes with increased collection time of nitrogen gas from the gas standard oven. Notice that the HCHO-oxime remains constant, indicating a better retention of this compound on the trap.

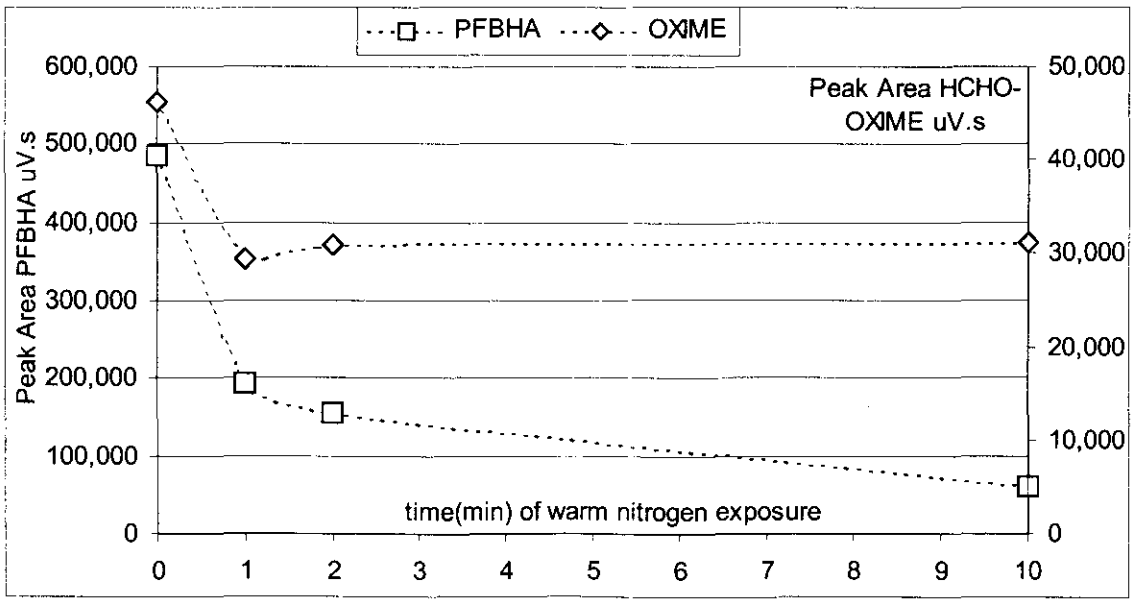

Figure 6.20. The depletion of PFBHA from the silicone trap with exposure to nitrogen at a flow rate of 10ml/min.

6.4 THERMAL DESORBTION – CRYOGENIC FOCUSSING

A description of the instrument was given in chapter 5. An experiment was performed to determine the conditions under which the HCHO-oxime would be completely transferred to the GC column i.e. when the desorption process is complete.
The silicone rubber trap, described in chapter 3, can be compared to a chromatographic column having a polydimethylsiloxane stationary phase. Literature [22, 50,129] and our own studies indicate that the HCHO-oxime elutes before the PFBHA. It could therefore be assumed that the PFBHA would "elute" off the silicone trap after the HCHO-oxime. Since no HCHO-oxime standard was available, determining the total transfer by using the PFBHA peak would have to suffice. (The alternative could also be to synthesise the HCHO-Oxime.)

However, after an initial exercise done by injecting PFBHA directly onto the column, it became clear that the PFBHA, being an amine, did not chromatograph well. Due to amine-interactions with the fused silica surface, tailing peaks were produced and not the ideal gaussian peak shapes required for normal integration. PFBHA would therefore be an unsuitable compound for quantitation.

Based on the above observations, we then decided to use dodecane (C12), which elutes after PFBHA. 1μL of a 20ng/μL C12 in CS_2, was placed onto the top of the silicone trap using a 5 μL syringe. As desorption flow is from the top to the bottom of the trap, once the C12 is completely desorbed it is obvious that any compound which elutes before C12 on the trap has also been completely desorbed. Traps were analysed using the TCT4020 HP GC-FID instruments, temperature program A, as shown in Table 6.1.

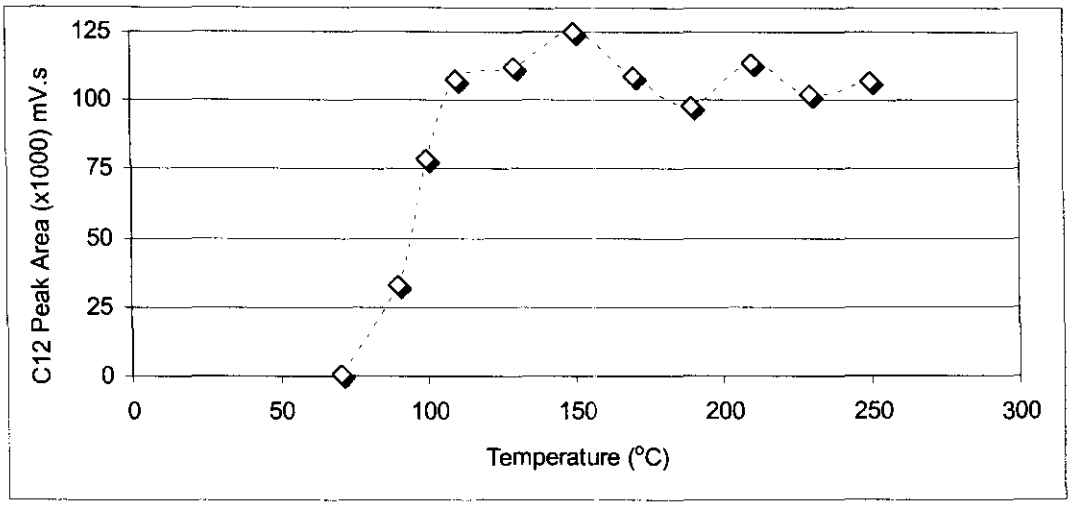

Figure 6.21. Optimisation of the thermal desorption of dodecane (C12) from a silicone trap

Figure 6.21, shows a graph of C12 peak area *versus* desorption temperature. From these results we can see that the C12 has reached a maximum peak area at 150 °C which is stable up to 250°C. A temperature of 220°C was chosen for the desorption process. Silicone degradation increases with higher temperatures, which result in increased silicone peak areas [26], causing additional problems such as peak overlap, column overload and contamination of the MS ion source. For this reason higher temperatures were not chosen. A blank run of the silicone trap after this desorption cycle indicates complete transfer of the oxime and reagent and no carry-over. We also decided to include a backflush cycle at 280°C for 10 min to remove any other compounds not desorbed at 220°C from the trap. In doing so we could ensure a clean, conditioned trap which is ready for use again.

Dodecane (C12) was added, as an internal standard, to all traps just before desorption in the TCT unit. The C12 was used not only to quantitate the amount of oxime formed, as described in section 5.3, but also as a means to check for any losses in the TCT unit during the desorption process.

6.5 REACTION EFFICIENCY

The ability of PFBHA to react with formaldehyde inside the silicone rubber was investigated. A linear increase of derivatised HCHO against collection volume would indicate that pre-concentration is occurring. The silicone rubber trap was loaded with pure PFBHA headspace for 10min at 5ml/min, followed by exposure to a HCHO-atmosphere for increasing time intervals, then analysed using the standard conditions described in table 6.1, temperature program A, TCT4020 HP GC-FID.
Two atmospheres were sampled: an 80ng/min HCHO gas standard provided a 5.98ppm HCHO atmosphere, and a 100ng/min HCHO gas standard sampled from the dilution system, described in chapter 4, yielded 1.33ng/min of HCHO which provided a 0.1ppm HCHO atmosphere.

Various exposure times were chosen in order to construct two curves of HCHO (ng) *versus* collection time. One curve is the plot of HCHO reacted against collection time, the other curve is the plot of HCHO flowing through the trap against collection time. The amount of HCHO reacted is calculated from the HCHO-oxime peak area and the peak area of the C12 internal standard, desorbed from the trap, using the method described in section 5.3.
The amount of HCHO flowing through the trap is determined based on the gravimetric measurement of the mass loss rate (ng/min) of the HCHO permeation gas standard and the calculated dilution factor (see chapter 4).

A comparison of the gradients of the two curves would indicate whether the reaction is 100% efficient or if it is below the expected mass loss rate of the HCHO gas standard. The assumption is made that no HCHO gas is lost in the set-up due to leaks, polymerisation or adsorption on surfaces in the set-up.

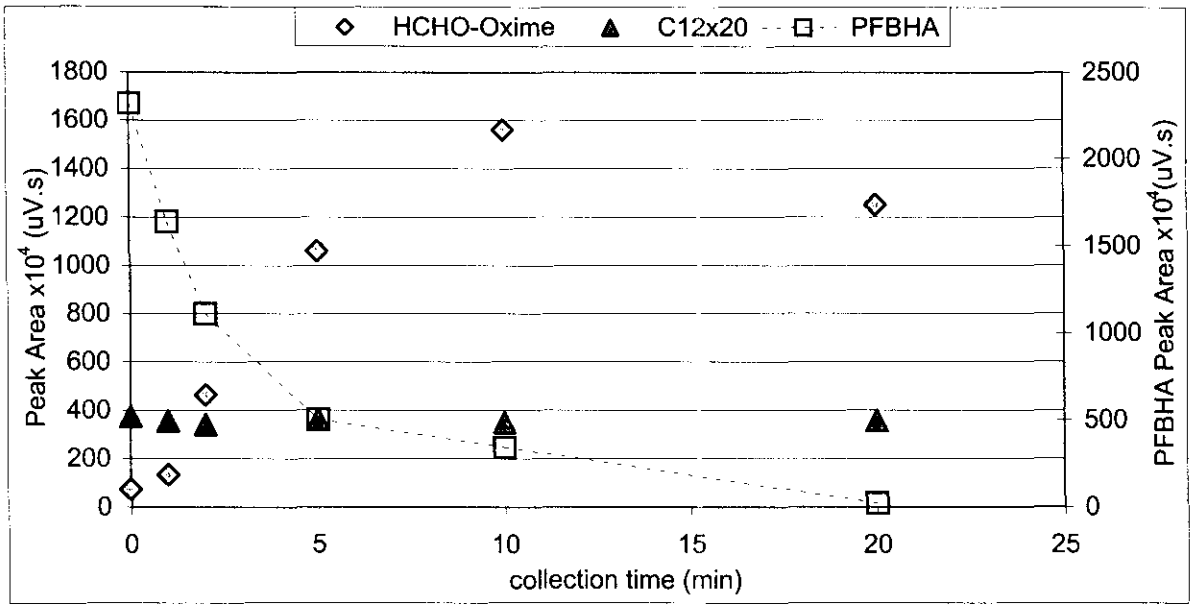

Figure 6.22. Collection of a 5.98ppm HCHO atmosphere at 10ml/min over time.

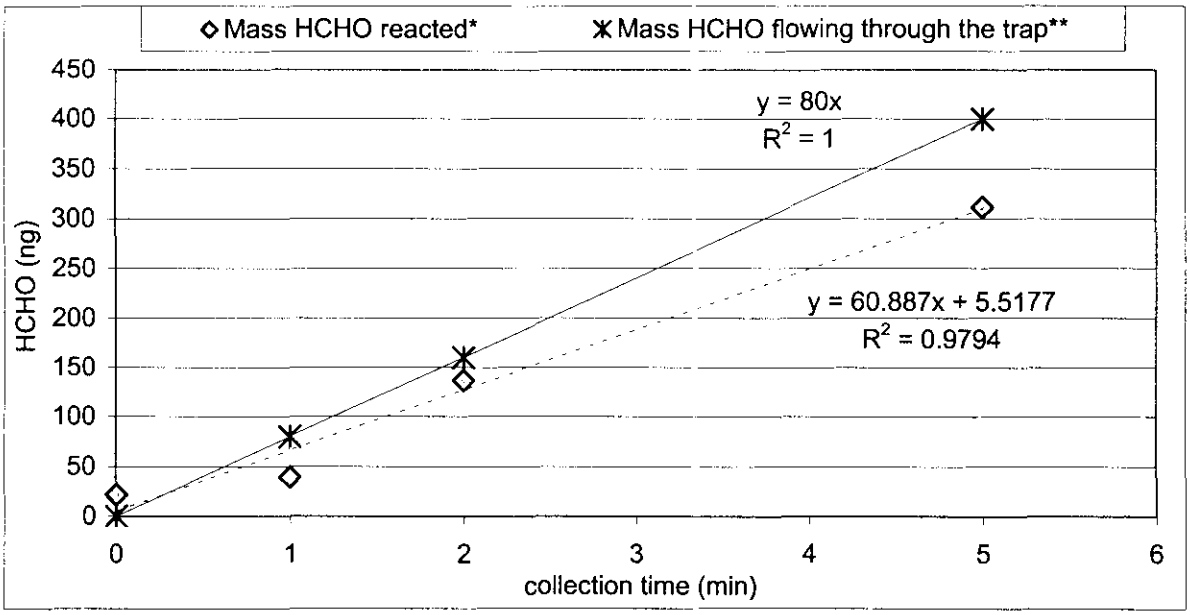

Figure 6.23. Determination of reaction efficiency of 5.98ppm HCHO with PFBHA.

*Mass of HCHO reacted is calculated with the HCHO-Oxime peak area (shown in Figure 6.22), the C12 internal standard peak area and relative response factor, using the method shown in section 5.3.

**Mass of HCHO flowing through the trap is determined from the gravimetrically measured mass loss rate (ng/min) of the HCHO gas standard sampled.

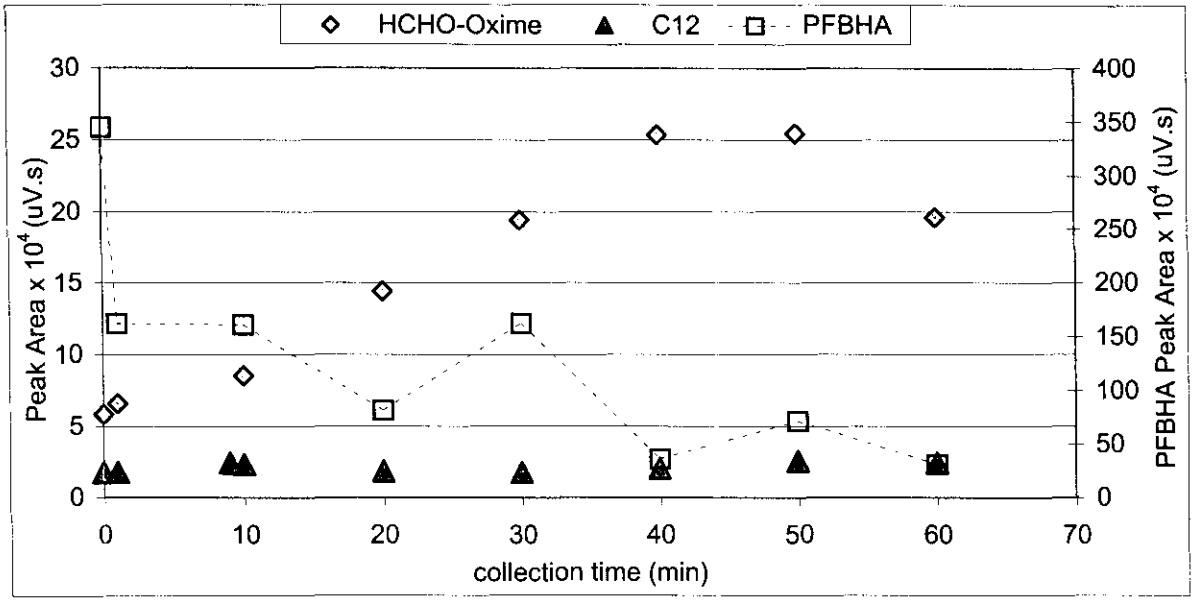

Figure 6.24. Collection of a 0.1ppm HCHO atmosphere at 10ml/min over time.

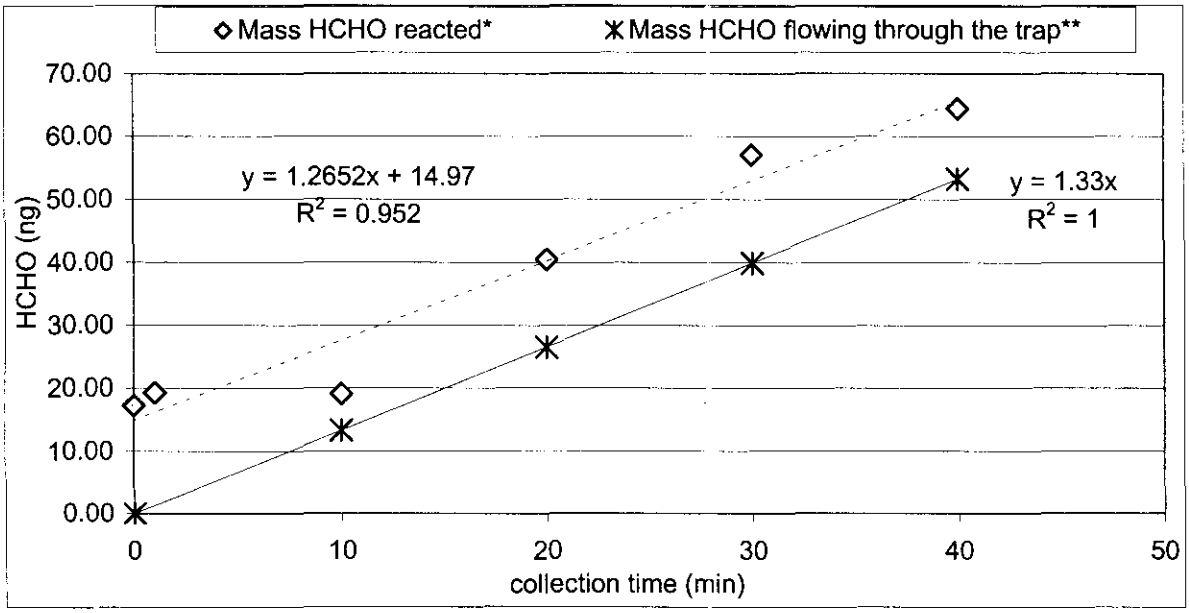

Figure 6.25. Determination of reaction efficiency of 0.1ppm HCHO with PFBHA.

*Mass of HCHO reacted is calculated with the HCHO-Oxime peak area (shown in Figure 6.24), the C12 internal standard peak area and relative response factor, using the method shown in section 5.3

**Mass of HCHO flowing through the trap is determined from the gravimetrically measured mass loss rate (ng/min) of the HCHO gas standard (and the calculated dilution factor) sampled.

Figure 6.22 shows the graph of peak area *versus* collection time, obtained for the sampling of a 5.98ppm HCHO atmosphere. Figure 6.23, shows the comparison of the gradients of HCHO (ng) reacted and HCHO (ng) flowing through the trap, for the first 60ml collected from the 5.98ppm HCHO atmosphere.

Similarly, figure 6.24 shows the graph of peak area *versus* collection time, for a 0.10ppm HCHO atmosphere. Figure 6.25 shows the comparison of gradients of HCHO (ng) reacted, and HCHO (ng) flowing through the trap, for the first 400ml collected from the 0.1ppm HCHO atmosphere.

Trapping from the 5.98ppm HCHO atmosphere (figure 6.22 and 6.23) shows a linear increase (R^2 = 0.9794) of the HCHO-Oxime peak area (figure 6.22) or the amount of HCHO reacted (figure 6.23), from 0 to 5 min collection time (50ml collection volume). Thereafter, the curve is no longer linear, and even starts to decrease, as the amount of PFBHA is depleted and therefore not available to react with the HCHO gas entering the trap. Thus trapping of concentrations above 5.98ppm, for longer than 100ml at 10ml/min, will not be quantitative. In addition, a comparison of the gradients (figure 6.23) indicates that the trapping is 75% of what we expected. Our HCHO gas standard provided HCHO gas flow through the trap at a rate of 80ng/min, but the HCHO was only being trapped (reacted) at a rate of 60ng/min.

Likewise, sampling of the 0.1ppm HCHO atmosphere (figure 6.24 and 6.25), indicates a linear increase (R^2 = 0.952) from 0 to 40 min (400 ml collection volume), then starts to decrease as PFBHA depletes. However, for this lower concentration, a comparison of the gradients in figure 6.25, indicates 95 % trapping efficiency during the first 400 ml collected. That is our HCHO gas standard provides HCHO gas flow through the trap at a rate of 1.33ng/min and this HCHO is being trapped at a rate of 1.26ng/min on our PFBHA-coated silicone rubber trap.

From these curves we are also convinced that our method to calculate the amount of aldehyde present, using Effective Carbon Numbers (ECN), the C12 internal standard and relative response factors, described in section 5.3, performs well.

This procedure was also applied to the other aldehydes in our study. Permeation standards of type 2 were used for acetaldehyde, propanal, acrolein and crotonal. Butanal and Benzaldehyde were type 1 permeation standards. Their respective permeation rates can be obtained from table 4.1. Figure 6.26, shows the chromatogram obtained for the sampling of the aldehyde permeation gas standards (type 2). These aldehydes were identified by their elution temperatures, obtained by the study above (section 6.2). Propanal, butanal and benzaldehyde were not detected.

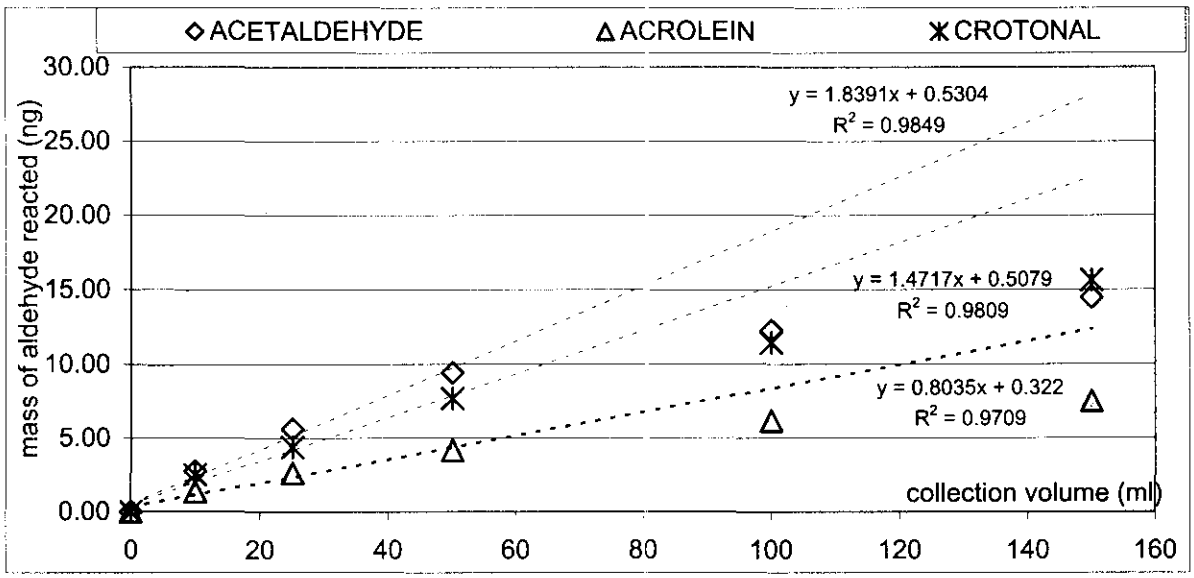

Figure 6.27. Determination of reaction efficiency of 3ppm acetal, 1.5ppm acrolein and 2.5ppm crotonal with PFBHA.

Mass of aldehyde reacted is calculated with aldehyde-oxime peak area, C12 internal standard and relative response factors using the method shown in section 5.3. The predicited ECN for acetaldehyde is 7.45, for acrolein 8.35 and crotonal 9.35.

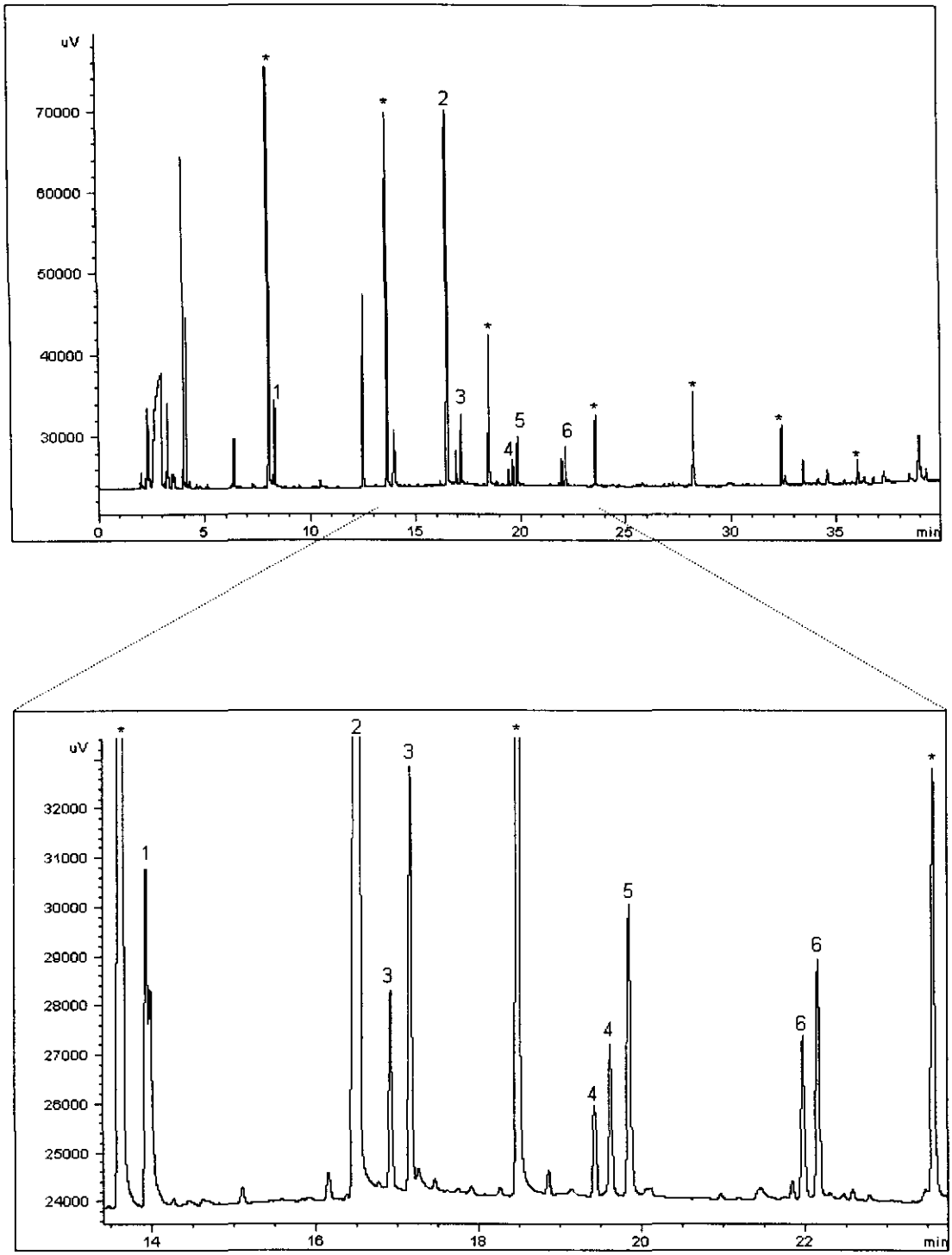

* Silicone peaks
1. Formaldehyde – oxime (from the PFBHA)
2. PFBHA
3. Acetaldehyde – oxime
4. Acrolein – oxime
5. 20ng C12
6. Crotonal - oxime

Figure 6.26 GC-FID chromatogram obtained for the collection of 3, 1.5 and 2.5 ppm acetal, acrolein and crotonal respectively, for 10 min at a flow rate of 10ml/min

Figure 6.27, shows the plot of reacted aldehyde over collection time for acetaldehyde, acrolein and crotonal at concentrations of 3, 1.5 and 2.5 ppm respectively, the dotted lines are the trend lines for the linear portions of each curve. In the first 5 minutes (50ml collection volume) there is a linear increase for each aldehyde, but upon comparison with the aldehyde amounts flowing through the trap (determined from the gas standards), they all indicate roughly a 4% reaction efficiency. It may be that these aldehydes do not react as rapidly with the PFBHA as HCHO does. However, we suspect that the gas standard glass impinger was not leak tight, and a more suitable leak-tight set-up should be made before further studies using these aldehydes are performed.

Based upon these results, table 6.3, lists the average percentage peak area of the first isomer peak to the second isomer peak, for acetal, acrolein and crotonal oxime. The ratio of these peaks appear to be constant, so in addition, this will allow for easier identification of the compounds when using an FID.

Table 6.3. The variation in the ratio of the isomer peaks of acetal, acrolein and crotonal-oximes.

	average % peak area 1 of peak area 2	%RSD	n
acetaldehyde-oxime	50.60	13.40	7
acrolein-oxime	59.38	8.31	6
crotonal-oxime	79.39	16.03	6

We also wanted to determine, based on these experiments, what would be the minimum detectable concentration of these aldehydes. For this calculation, using the results from the 1 min (10ml) collection of the permeation standards, we obtained the signal-to-noise (s/n) ratio of the second isomer peak of the aldehyde-oximes. We then

solved for the minimum concentration that can be detected at a s/n ratio of 3. Table 6.4 shows the minimum detectable concentrations for acetaldehyde, acrolein and crotonal. From these results, we are content to see that the detection limits we obtained for these aldehydes are below their Permissible Exposure Limits (PEL) [6]. In addition, we know that these results are based on a sample collection time of only 1 min, therefore a longer sample collection time would result in even lower detectable concentrations.

Table 6.4. Determination of minimum detectable concentrations for acetaldehyde, acrolein and crotonal.

	acetal	acrolein	crotonal
Permissable Exposure Limit (ppm) [6]	100	0.1	2
gas standard concentration (ppm)	3.0	1.5	2.5
s/n isomer peak 2	257.7	79.1	118
minimum detectable concentration (ppm) at s/n 3	0.035	0.057	0.064

6.6 REAGENT DEPLETION *versus* BREAKTHROUGH VOLUME

In chapter 3, we discussed the retention capability of a sorbent trap in terms of its breakthrough volume. In this study two silicone traps, coated with PFBHA, were arranged in series. The first trap remained at the outlet of the 0.1ppm HCHO atmosphere, while the second trap was analysed for breakthrough. The second trap was replaced each time with a new PFBHA coated trap. All traps were analysed as in section 6.5. FID range was 2^0. Figure 6.28, shows the curve obtained for a

breakthrough study of HCHO and its derivative. All data points are obtained from the analysis of the second trap, except for the last data points (after 3000ml) for the HCHO-oxime and the PFBHA which, are from the first trap.

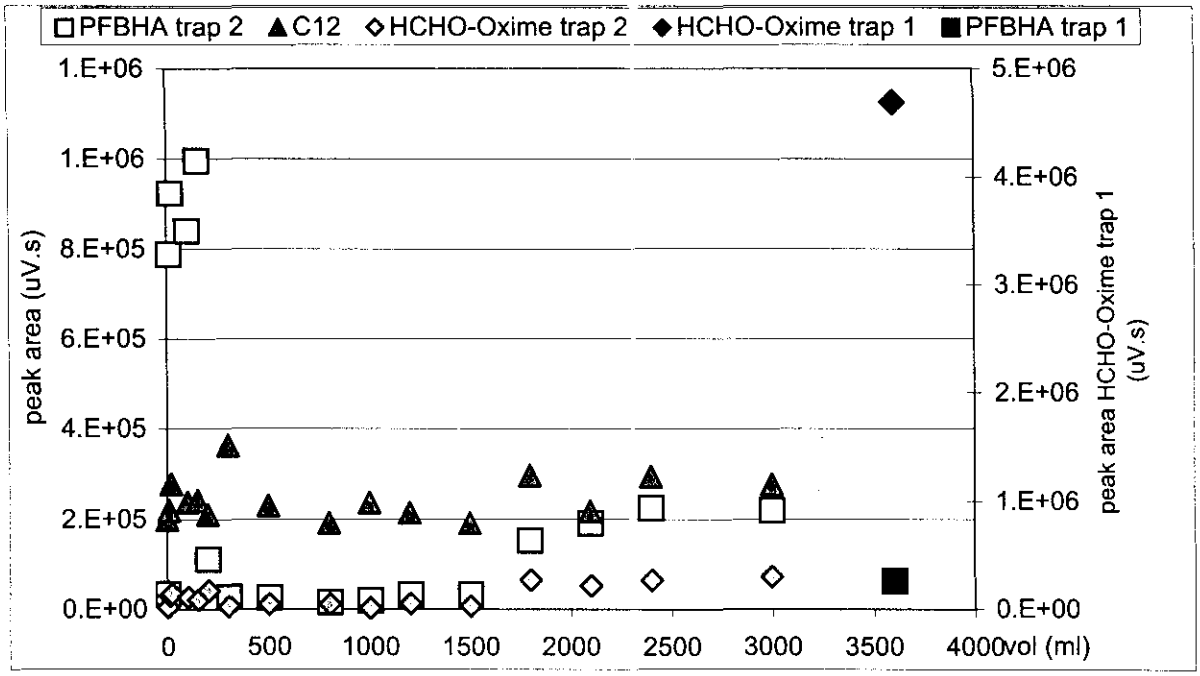

Figure 6.28. Determining the breakthrough volume of the HCHO-oxime onto the second trap*.

*Two PFBHA-coated traps were arranged in series at the exit of the 0.1ppm HCHO atmosphere. The second trap is analysed after the various collection volumes indicated. Collection flow rate 10ml/min.Dodecane (C12) is the internal standard. Data points after 3500ml were obtained from the first trap.

After 3 litres of sampling, we expected some breakthrough onto the second trap, as surely the PFBHA would be depleted on the first trap at this time, as discussed above in section 6.5. The slight increase of HCHO-oxime from 1800 ml onwards we attribute to the proportional increase in PFBHA loaded on the second trap.

Since there was no clear increase of HCHO-oxime on the second trap, the HCHO was still being retained somehow. Upon desorbing the first trap, it was clear that there was no breakthrough of HCHO-oxime, even after 3 litres of sampling. The PFBHA was still present on the first trap, but no longer in excess as seen in figure 6.28.

From this curve, it is clear that the HCHO-oxime is well retained on the trap. Nevertheless, of greater importance is the depletion of the PFBHA. We suspect that once the reagent is totally consumed on the first trap, breakthrough of HCHO will occur. It is possible that some HCHO, not efficiently trapped by the depleting PFBHA on the first trap, could have broken through but that it never exceeded the background HCHO amount in the reagent on the second trap.
Since the HCHO-oxime is well retained on the silicone trap, we can also deduce that the other aldehyde-oximes, which elute after the HCHO-oxime, will have an even better retention on the silicone rubber trap.

6.7 CONCLUSION

From these studies, we can conclude that *in-situ* derivatisation on silicone rubber traps is possible. A simpler method is used for coating the sorbent with derivatising reagent, which effectively reduces sample preparation time. Aldehydes are pre-concentrated and retained on the silicone by reacting with the PFBHA in the silicone to form the stable oxime products. These products have been successfully desorbed from the silicone rubber trap and analysed by Flame Ionisation Detection and Mass Spectrometry.

However, our biggest problem remains the high formaldehyde-oxime contamination in the PFBHA reagent. In addition, the reagent cannot be loaded onto the silicone rubber trap with high repeatability. Consequently, our next step in this project, is to investigate possible methods such as recrystalisation [50] to eliminate these problems as it severely restricts our detection limit for HCHO. HCHO atmospheres as low as 0.1ppm has been detected. This detectable amount does meet certain exposure limits

set by OSHA, ACGIH and the WHO, shown in table 1.1, but not the NIOSH PEL of 0.016ppm.

We have shown that permissible concentration exposure limits for acetaldehyde, acrolein and crotonal can be reached with our method (table 6.4). Lower detection limits are possible for these aldehydes as they are not present in the reagent blank. For this reason we could have loaded more PFBHA onto our silicone rubber traps for the determination of the reaction efficiency of these aldehydes with PFBHA, and for determination of their minimum detectable concentrations. However, further work is required on the gas standard set-up, as a leak was suspected.